V. PHYSICAL ACOUSTICS*

Academic Research Staff

Prof. K. U. Ingard

Graduate Students

C. M. Christensen
A. G. Galaitsis
J. A. Tarvin

A. EFFECTS OF GEOMETRICAL ASYMMETRIES ON THE BEHAVIOR OF AN ORIFICE

At high enough levels >130 dB sound interactions become nonlinear. Nonlinearities arise either from flow separation[1] that normally occurs on the downstream side of sudden duct constrictions or from quadratic terms[2] that would justifiably be omitted at low levels.

In this report we study a nonlinear effect introduced by the geometric asymmetry of an acoustic element interacting with a sound field. The element is a metal plate P with an orifice O of rectangular cross section whose area has a minimum value $A_m = 0.8\ cm^2$ on one side of the plate and a maximum value $A_x = 4.5\ cm^2$ on the other side (Fig. V-1). Because of this directional asymmetry, the orifice impedance will

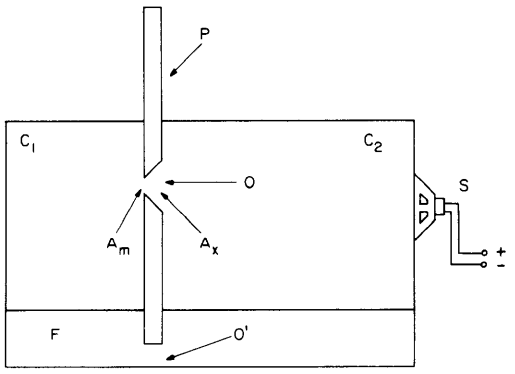

Fig. V-1.
Experimental arrangement.

take on different values for opposite direction of flow, and therefore a sinusoidal pressure drop across the plate will produce a partially rectified acoustic velocity in the constriction. We shall present experimental evidence of such behavior, and give a simple analysis predicting the frequencies at which this phenomenon can best be observed.

*This work was supported principally by the U.S. Navy (Office of Naval Research) under Contract N00014-67-A-0204-0019.

1. Experimental Arrangement and Observations

A rectangular box (Fig. V-1) with inner dimensions D_1 = 16.2 cm, D_2 = 4.0 cm, and D_3 = 8.1 cm was made of plexiglas, 0.5 in. thick, and was divided into compartments C_1 and C_2 by means of an aluminum partition, 5 mm thick, with an asymmetric orifice as described above. The two compartments C_1 and C_2, L_1 = 5.1 cm and L_2 = 10.6 cm long, respectively, communicate through the orifice O, as well as through an opening O', 4 mm wide, at the base of the partition. The cavity, which is excited by an Atlas sound driver S, is partially filled with fluid F to a height h ~ 2.5 cm. The fluid, which serves as a detector of the time average pressure drop across the plate, rises in C_1 and drops in C_2 when ν_1 = 650 Hz, as shown in Fig. V-2a. The partition is then removed from the slot, rotated 180° about its vertical axis, and reinserted into the cavity while the frequency and intensity of the sound are kept constant. The result is shown in Fig. V-2b. The higher fluid level in C_1 (Fig. V-2a) implies lower pressure in C_1 or equivalently a net transfer of air from C_1 to C_2. The situation in Fig. V-2b shows the effect of reversing the orifice plate, which favors flow from C_2 back to C_1. As the frequency is varied, the effect becomes weaker and it disappears below 400 Hz or above 950 Hz. The next frequency at which the same behavior is encountered is in the vicinity of ν = 1460 Hz. This phenomenon can best be observed at certain resonance frequencies when the acoustic velocity in the orifice is in the vicinity of a maximum, in which case the interaction becomes stronger and the effect is amplified.

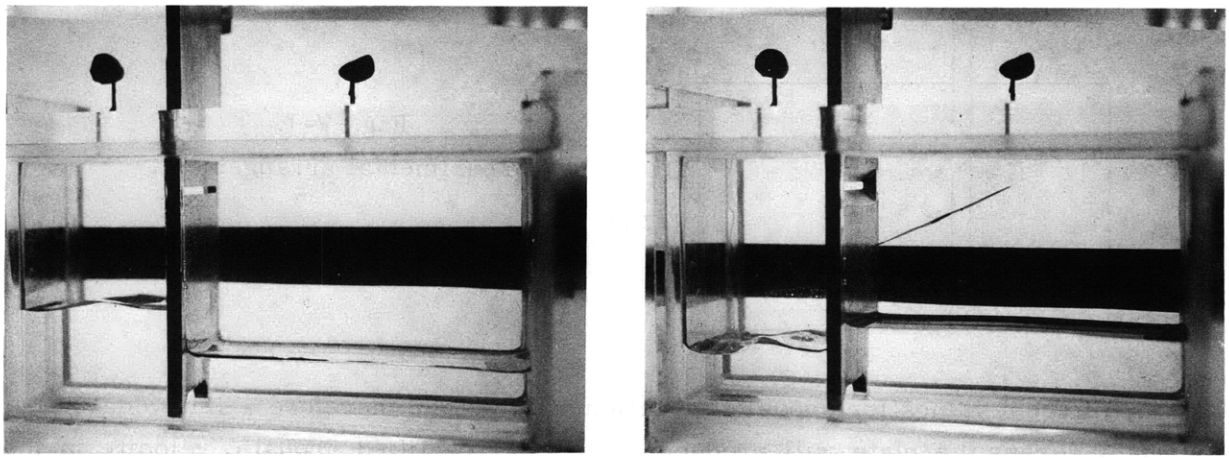

Fig. V-2. Demonstration of the dependence of the average pressure drop across the orifice plate on the orientation of the orifice plate. ν_1 = 650 Hz. Sound level = 151 dB in the C_1 compartment. Preferred direction of flow (a) to right (b) to left.

2. Calculation of the Resonance Frequencies

The analysis of this problem in complete form is difficult because of the presence of nonlinearities. It is possible, however, to estimate the resonance frequencies if we ignore nonlinear contributions and apply the procedures of linear theory. We further assume that the sound waves are plane waves (and parallel to the orifice plate) in which case the response of the system can easily be derived by working with its electric analog, as shown in Fig. V-3. The source, S', of strength $p = p_o e^{-i\omega t}$, produces a response $U = U_o e^{-i\omega t}$ in ζ_o, where $\zeta_o = \theta_o - i\chi_o$ is the impedance[3] of the orifice; $\zeta_2 = i \cot \alpha x$ is the impedance of compartment C_2; and $\zeta_1 = -i \tan (x/2)$ and $\zeta_3 = i/\sin x$ are impedances contributed by C_1, where $x = kL_2$, with k the wave vector and $\alpha = L_1/L_2$.

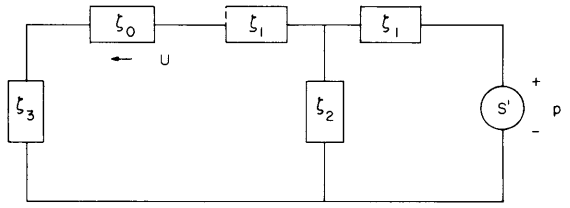

Fig. V-3. Electric analog of the acoustic system shown in Fig. V-1.

Maximizing the acoustic velocity u_o at the orifice is equivalent to maximizing the amplitude of the current $U = U_o e^{-i\omega t}$, given by

$$\frac{U_o}{p_o} = \frac{\zeta_2}{(\zeta_1+\zeta_2)\zeta_R + \zeta_1\zeta_2} = \frac{1}{\theta_o \cos x - i(\chi_o \cos x + \sin x - \cos x \cot \alpha x)} \equiv \frac{1}{Q}$$

or minimizing the magnitude of Q. The real part of Q is always less than θ_o, but the imaginary part blows up periodically because of the presence of the term $\cot \alpha x \cos x$. Consequently, the minima of Q should be in the vicinity of the minima of Im (Q) which we calculate from

$$\chi_o = \cot \alpha x - \tan x.$$

The functions $y_1 = \chi_o = kt'/\sigma$ and $y_2 = \cot \alpha x - \tan x$ are plotted in Fig. V-4. $\sigma = A_o/A_1$, where A_o, A_1 are the cross sections of the orifice and the compartment C_1, respectively, and t' is the effective thickness of the orifice.[3] y_1 is plotted for four different values of σ that range from $\sigma_m = 0.04$ corresponding to $A_o = A_m$ to $\sigma = 0.20$ corresponding to $A_o = A_x$. For $\sigma = 0.04$ we obtain $\nu_1 = 520$ Hz and $\nu_2 = 1520$ Hz. In view of all of the approximations made to obtain these values, the discrepancies are not surprising. A more rigorous derivation should provide for an asymmetric current U, and should also allow this asymmetry to disappear as $A_x \rightarrow A_m$, or as the thickness of the

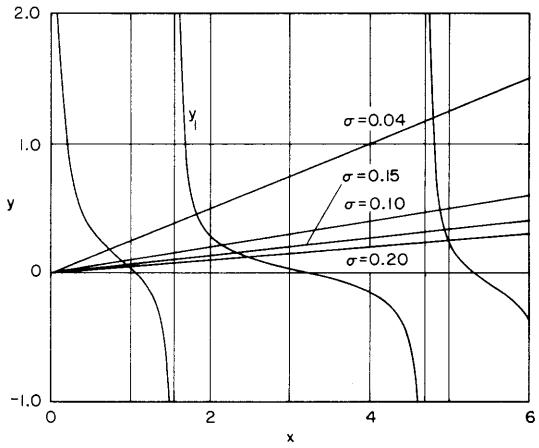

Fig. V-4. The functions $y_1 = \cot \alpha x - \tan x$, and $y_2 = kt'/\sigma$. $\sigma = A_o/A_1$, where A_o is the cross section of the orifice and A_1 is the cross section of C_1. $y_1 = y_2$ gives approximate values of the resonance frequencies.

orifice, t', goes to zero, or as A_x becomes much larger than A_m.

The experiment was repeated with different values of A_x, A_m, and A_m/A_x and the following results were established: (a) the asymmetric orifice behaves like a rectifier; (b) the direction in which the flow is favored is from A_x to A_m; and (c) the rectification is stronger when the smallest dimension of the orifice is of the same order as its thickness or less.

A. G. Galaitsis

References

1. S. Whitaker, Introduction to Fluid Mechanics (Prentice-Hall, Inc., Englewood Cliffs, N.J., 1968).
2. U. Ingard and D. Galehouse, Am. J. Phys. 39, 811-813 (1971).
3. U. Ingard, J. Acoust. Soc. Am. 25, 1037 (1953).

B. NONLINEAR ATTENUATION OF SOUND IN DUCTS

The level of sound propagating in a duct can be reduced through the use of absorbing walls, usually made of perforated facing backed by acoustic resonators.[1,2] At low intensities this results in a linear decrease of the sound pressure level (SPL) with distance from the source. This dependence changes, however, at high levels because the interaction of sound with the absorbing boundaries becomes nonlinear.[3]

The characteristics of sound propagation in such a duct were studied and measured

values of the attenuation coefficient and the phase velocity as a function of frequency and SPL are presented.

1. Experimental Arrangement and Measurements

The test duct and a block diagram of the electronic equipment are shown in Fig. V-5. Sound generated by the driver S propagates through the duct D, 40 cm long, and the test section T, 170 cm long. The duct cross section is 3/4 in. wide and 7/8 in. high. In the test section the upper wall of the duct is replaced by a sheet, 1/8 in. thick, with circular orifices of radius 1/8 in. with a 1-in. spacing. Each orifice is backed by an acoustic resonator 3/4 in. in diameter and 1 in. deep. The porous termination A greatly reduces reflection from the far end, especially for $\nu > 750$ Hz. The 1/4 in. probe microphone is mechanically coupled to a 10-turn potentiometer P whose arm voltage varies linearly with the position x of the probe tip. The x = 0 point was chosen 5 cm inside the test section.

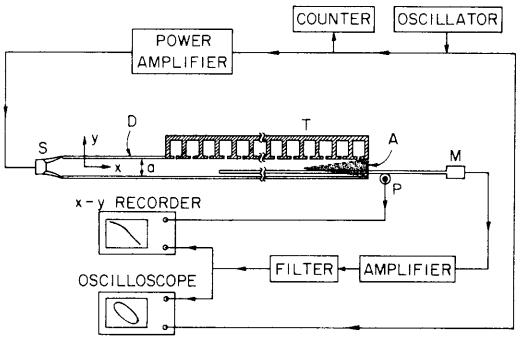

Fig. V-5. Test arrangement for measurement of the attenuation coefficient Q and the phase velocity C_p.

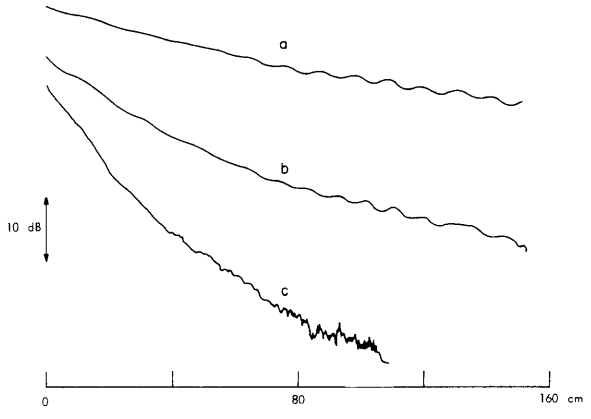

Fig. V-6. Typical traces of sound pressure level vs distance x in the duct. (a) ν = 1005 Hz. (b) ν = 1105 Hz. (c) ν = 1198 Hz.

If the x dependence of the sound wave is $e^{ik_1 x - \gamma_1 x}$, we define the attenuation coefficient Q and the phase velocity C_x by

$$Q = 20\, \gamma_1 \log e$$

$$C_x = \frac{2\pi\nu}{k_1}. \qquad (1)$$

Q is obtained by measuring the tangent to the SPL vs x graph which is plotted on the x-y recorder. C_x is calculated from (1) and $k_1 = 2\pi/\lambda_x$ after λ_x has been measured through construction of Lissajous figures.

Typical SPL vs x traces are shown in Fig. V-6. The level is 150 dB at x = 0 for each trace. The attenuation becomes stronger and the deviation of the traces from a

straight line increases close to the first resonance, ν = 1371 Hz, because the acoustic velocity in the constrictions approaches a maximum value which favors greater energy dissipation and amplifies the nonlinear characteristics of the interaction.

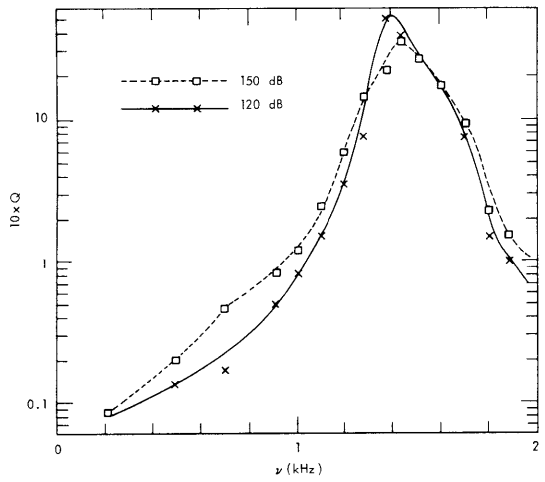

Fig. V-7. Measured values of the attenuation coefficient Q.

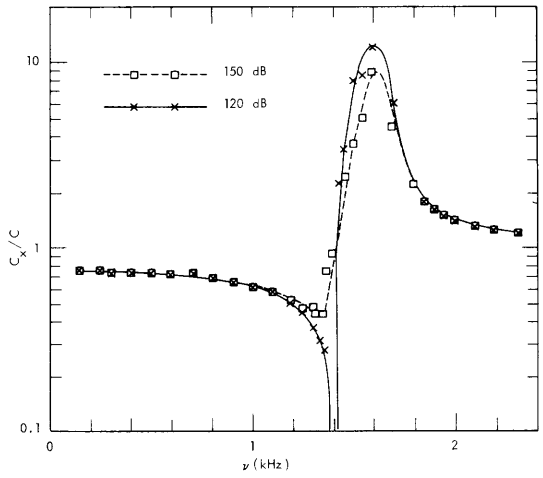

Fig. V-8. Measured phase velocity C_p.

Figure V-7 shows Q vs frequency at levels of 120 dB and 150 dB. $Q_{120} > Q_{150}$ in the vicinity of resonance, which is not surprising because it is expected that the orifice flow will be choked at higher levels and this lowers the dissipation rate.

The results of the phase-velocity measurements are shown in Fig. V-8. C_{120}/C and C_{150}/C are plotted against ν, where C_{120}, C_{150} are the phase velocities along the duct at 120 dB and 150 dB, and C is the free-field phase velocity. The accuracy is reduced in the vicinity of resonance because the attenuation is so strong and/or the phase velocity so great that the measured phase changes only by a small fraction of 360°, even when the microphone is moved through a distance that results in a drop of as much as 30 dB in SPL. In this region the phase measurements were performed as suggested in the oscilloscope manual.[4] Greater accuracy can be obtained through the use of more sophisticated correlators.

The dynamic range of C_{120} is quite striking, and extends from practically zero (at ν = 1373 Hz and ν = 1400 Hz, both of which fell outside the lower margin of the frame) to approximately 12x C at ν = 1600 Hz. The effects of resonance are more pronounced for C_{120} than for C_{150} which indicates a higher absorption at lower levels, in agreement with the plots in Fig. V-7.

We are now studying a theoretical model that will enable us to predict the values of Q and C_x. We expect to present the results, as well as more data

on different sized test sections, in a future report.

A. G. Galaitsis

References

1. U. Ingard and D. Pridmore-Brown, J. Acoust. Soc. Am. 23, 589 (1951).
2. U. Ingard, J. Acoust. Soc. Am. 26, 151 (1954).
3. U. Kurze and C. Allen, J. Acoust. Soc. Am. 49, 1643 (1971).
4. Type 555 Cathode-Ray Oscilloscope Instruction Manual (Tektronix Inc., Beaverton, Oregon, n.d.).